Control of directivity of PVDF hydrophones using anisotropic substrates

Andrew Munyard[1] and David Matthews[1,2]

[1]Defence Science and Technology Group
[2]School of Mechanical & Chemical Engineering, University of Western Australia, Perth, Australia

ABSTRACT

Development of a compact underwater sound intensity sensor based on the "two hydrophone" (or 'p-p') principle would be very useful for many underwater applications. Attempts to develop sound intensity probes based on the combination of particle velocity and pressure sensors have been reported by some authors but their suitability for use on a moving platform is unconvincing. Our previous work focused on using piezoelectric PVDF polymer films to construct such a p-p sound intensity sensor. This showed some promising results but difficulties arose in compensating for the directivity of the individual pressure sensor films. Ideally these should be omni-directional in order to accurately estimate the sound pressure gradient using the finite difference approximation. By using anisotropic backing materials it has been possible to control the directionality of the PVDF films up to frequencies as high as 50 kHz. The effect of various substrate anisotropies on the directionality is discussed.

1. INTRODUCTION

Piezoelectricity in Polyvinylidene Fluoride (PVDF) was discovered by Kawai in 1969 (Kawai, 1969). Since then many underwater applications have been reported in the literature. Like ceramic piezoelectric materials PVDF is also highly anisotropic. As a result the piezoelectric voltage generated from an impinging acoustic pressure will depend on the mode of vibration of the PVDF film. This mode of vibration depends not only on the wavelength of the acoustic pressure but also on how the film is physically constrained. Complications arise from the fact that it is necessary to encapsulate the piezo-element in some sort of protective material such as polyurethane. Ideally this material should have an acoustic impedance closely matching that of water. Since PVDF is a thin flexible film it is also necessary to use some form of support material to hold the film in position during the fabrication process. Both of these factors have significant effects on the sensitivity and directivity of the final sensor.

A number of papers have reported on various PVDF hydrophone designs that try to optimize the sensitivity by manipulating things such as hydrophone shape (Ricketts, 1980), pressure release systems (Holden et al., 1983) anisotropy control (Bhat, 1995). A detailed review of much of this work has been given by Khart (Khart, 2007). However, less work has been reported on the control and understanding of the directivity of PVDF hydrophones. Of those that have, the majority focuses on ultrasonic applications and much less in the lower frequency region applicable to sonar. Moffett (Moffett, 1986) reported on the construction and characterization of a ρc hydrophone using PVDF film in the frequency range 50 kHz < f < 100 kHz. He successfully modeled the directivity of the flexural plate hydrophone using a piston set in a rigid baffle. This however was done at a single frequency of 100 kHz. It was later shown (Matthews et al., 2013) that for similar PVDF hydrophones, this model was only capable of modeling certain frequencies in the range 30 kHz < f < 100 kHz and many of the observed features were not explainable using this model. Similar discrepancies have been reported by Woodward (Woodward & Chandra, 1978) and were attributed to the collimating effect of the transducer holder.

In previous work (Munyard et al., 2012) we have shown the effect of using a glass fibre substrate to increase the omni-directionality of PVDF hydrophones in the frequency range 30 kHz < f < 100 kHz. Similar measurements done using Aluminium backing material showed little differences (Munyard et al., 2012). In this paper we present some additional results on our investigations into this phenomena by controlling the direction of the fibers relative to the orientation of the PVDF film. In doing so it was possible to introduce an anisotropic Young's modulus into the substrate which, in turn affects the directivity of the planar films.

2. THEORY

Piezoelectric PVDF films generate a voltage that depends on the applied stress. Due to the anisotropy of the material, coefficients are assigned for each direction of the piezoelectric film. The specific values are then indexed X_{nm} where **n** corresponds to the direction of polarization and **m** corresponds to the direction of the mechanical stress. The axes definition for the piezo-film is shown in Figure 1 where the 1,2 and 3 directions lie parallel to the length (l), width (w) and thickness (h) of the film respectively. The films used in this report were polarized in the 3 direction with the electrodes placed on the surface of the film. As a result n = 3. For example a 33 index will correspond to a value for the voltage generated between the two large faces of the film (3 direction) for a stress applied in the 3 direction.

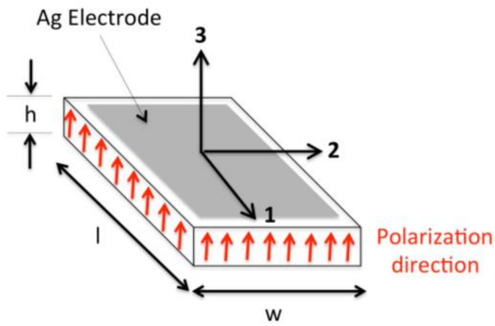

Figure 1. Axes definition for piezoelectric films

For a PVDF film of thickness h polarized in the 3 direction, subjected to an applied stress T, the free field voltage V_o is given by;

$$V_o = g_{31}T_1h + g_{32}T_2h + g_{33}T_3h \quad (1)$$

where g_{31}, g_{32} and g_{33} correspond to the piezoelectric stress constants in the 1,2 and 3 directions and T_1, T_2 and T_3 corresponds to the applied stress in the three directions. Most available low to mid-frequency hydrophones available will operate in one of three modes depending on the method of construction and the operational frequency. These are;

- 31 Mode. The stress is applied along 1 direction and the other two axes are free to move. In this case the free field voltage output is given by $V_{31} = g_{31}T_1h$
- 33 Mode. This is the simplest case mode where the stress is applied in the 3 direction and the other two directions are free to move. In this case the free field voltage output is given by $V_{33} = g_{33}T_3h$
- Hydrostatic Mode. All three axes are clamped. This is more applicable to sensors that have been encapsulated in polyurethane such as the ones reported here. The voltage output is given by $V_h = g_hh$ where $g_h = g_{31} + g_{32} + g_{33}$

PVDF, like many of its ceramic counterparts, has a negative stress constant in the 3 direction and positive components in the other two. Hence, when operating in hydrostatic mode, the overall result is a reduction in the total g_h constant. For the SDT1 films used in this paper g_{31}= 0.216 V.mN^{-1}, g_{32} = 0.003 V.mN^{-1} and g_{33} = -0.33 V.mN^{-1} . Despite this, its hydrostatic mode response is still significantly larger than PZT ceramics.

As can be seen from equation (1) the output voltage is controlled by the individual stress constants T_n (n=1,2,3). These are related to the material that the acoustic pressure propagates through and, as a result, it is possible to control these values by a suitable choice of substrate material. For a pressure wave acting on the polyurethane cylinder the output voltage of the sensor will be the voltage generated due the average stress experienced by the PVDF element in each of the directions 1,2 and 3.

For the measurements discussed in this paper the 1 direction of the film is parallel to the axis of rotation of the sensor. As a result the contribution of V_{31} to the output of the sensor is constant and independent of θ. Consequently the angular variation of the sensor output will depend on the contributions of V_{33} and V_{32} which in turn depend on the stresses in these two directions (T_3 and T_2). It has been shown (Kotian et al., 2013) that the stress experienced by the sensor T_{PVDF} and the stress in the substrate T_{sub} is related by the ratio of the Young's moduli,

$$T_{pvdf} = \frac{E_{pvdf}}{E_{sub}} T_{sub} \tag{2}$$

Where E_{pvdf} and E_{sub} is the Young's Modulus of the PVDF film and substrate respectively.

If the applied force is in the 3 direction then the Young's modulus of the substrate will be the same regardless of whether the fibres are parallel to the 1 or 2 direction (for both orientations the applied force is perpendicular to the fibres). In the 2 direction however the Young's modulus will depend on whether the fibres run parallel or perpendicular to the 2 direction. The highest Young's modulus will occur when the fibres run parallel to the applied force (Wang et al., 2013). From equation (2) it can be seen that an increase in the Young's modulus in the substrate will result in a reduction in the stress in the PVDF film. This will reduce the contribution of V_{32}. As mentioned above, g_{33} is negative and g_{32} is positive. A reduction of V_{32} will therefore result in an increase in the overall sensitivity of the sensor given by equation (1).

The absolute receiving response (M_H) of the sensor is the open circuit voltage (V_o) generated by a plane wave of unit pressure (P) and is expressed in V/Pa.

$$M_H = \frac{V_o}{P} \tag{3}$$

The open circuit sensitivity of the hydrophone, M_o (dB re 1V/μPa) is given by;

$$M_0 = 20log|M_H| - 120 \tag{4}$$

3. EXPERIMENTAL SETUP

3.1 Sensor Construction

SDT1-D28 films were used as the active piezo-material for all sensors discussed in this report. These were obtained from Measurement Specialties Inc. They are PVDF films that have been folded to reduce EM noise and have an active area of 13 mm by 30 mm. They have a thickness of 28 μm and have been polarized in their thickness direction. The 1 and 2 directions are parallel to the length and width of the film respectively. The films are supplied with shielded cables and were terminated with a SMB connector.

To construct sensors SDT1 films were laminated between two layers of carbon fibre or glass fibre fabric using a standard vacuum bagging technique. Two fabric types were used; unidirectional carbon fibre (CF) and biaxial glass fibre (GF) ±45°. The unidirectional CF was placed parallel to and at 90 degrees to the 3-1 direction of the film. The biaxial GF had the fibres at 45° to the 3-1 direction. In addition to these "backed" sensors a freestanding SDT-1 reference sensor was also constructed.

The vacuum bagging technique requires the use of a fabric during the construction phase. For this work 'wet out' was used in conjunction with West System 105 epoxy resin and 205 fast hardener catalyst. All sensors were constructed on a sheet of glass by sandwiching a SDT1 film between a top and bottom layer of CF of FG fabric. Peel ply was placed over the sensor laminate and a vacuum bag added allowing for the application of 1 bar of vacuum. The vacuum was maintained until the resin had solidified.

Once cured and hard, the peel ply was removed and the sensors trimmed to a size of 25mm wide by approximately 50mm long. A cylindrical mould was used to cast Scorpion Oceanics Sol-Res 01 polyurethane around the sensor to provide waterproofing and impedance matching to water. The sensor was held in the mould by supporting one face with sticky tape and taping to the mould flange. This results in a slight offset of the sensor from the central plane by half the sensor thickness. A threaded brass insert was moulded into the top of the sensor to facilitate mounting in the test tank. The encapsulated sensor measured 30mm diameter by approximately 90 mm long. A schematic of a typical sensor is shown in Figure 1.

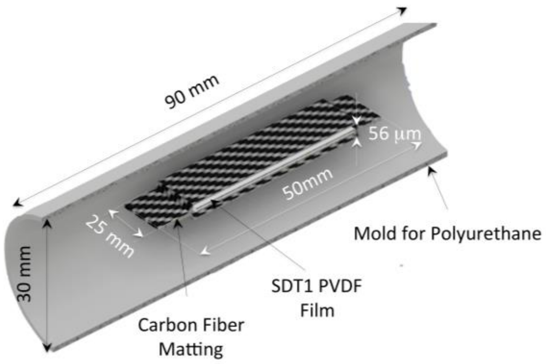

Figure 2. Schematic of a typical sensor using a SDT1 piezo-film. The film is shown in white and is sandwiched between two pieces of carbon/glass fibre.

A list of sensors discussed in this report is shown in Table 1 below. Sensor #1 was a plain SDT-1 film with no backing material and was used for comparison.

Table 1. List of the PVDF sensors constructed and discussed.

Sensor #1	Plain SDT 1 film. No backing material
Sensor #2	Carbon Fibre lengthways. Parallel to the 1 direction
Sensor #3	Carbon Fibre athwart. Parallel to the 2 direction
Sensor #4	Glass Fibre bi-axial, +/- 45^o

3.2 Sensor Characterisation

Sensors were calibrated in a small fresh water tank of diameter 1.8 m and depth 1.0 m. They were placed at a distance of 0.445 m from the centre of the tank and at a depth of 0.5 m. An ITC 1042 transmitter was placed at the same depth in the centre of the tank and a Reson 4015-5 reference hydrophone placed co-linearly on the opposite side of the PVDF sensor at a depth of 0.5 m and a distance of 0.445 m from the sound source. A diagram of the setup is shown in Figure 3. By using this arrangement it gives a delay time of 0.43 ms (assuming a sound speed of 1500 ms^{-1}) between the direct and reflected paths from the surface, bottom and sides.

An Agilent 33220A signal generator and an Agilent 33502A voltage amplifier with 25-times gain was used to drive the ITC 1042. The output from the PVDF sensors were conditioned using a Stanford SIM910 JFET preamplifier set to a gain of 100 together with a Stanford SIM965 filter using a 1Hz high pass filter and a 200 kHz low pass filter. The output from the sensor was monitored using an Agilent DSO1024A 200 MHz oscilloscope.

The sensitivity of the sensors was measured for the frequency range 30 kHz $\leq$ f $\leq$ 100 kHz in increments of 10 kHz. The lower limit was constrained by the dimensions of the tank as discussed above. The directivity of the PVDF sensor was measured by rotating the sensor from 0 to 360^o. The output of the films were measured every 10^o.

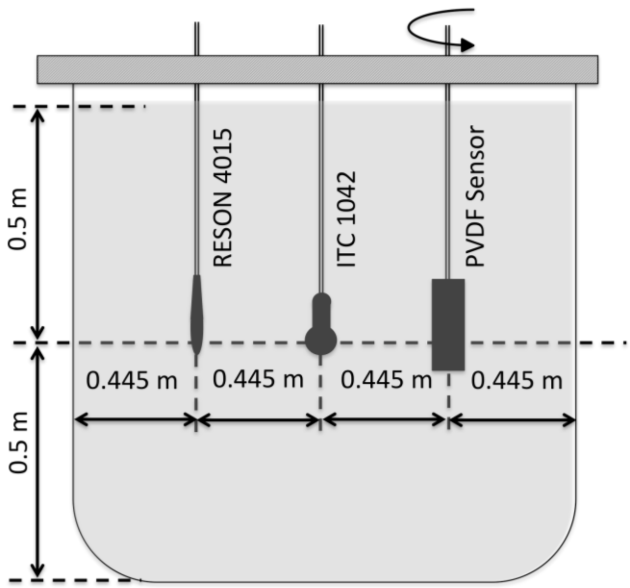

Figure 3. Setup for calibrating PVDF sensors

4. RESULTS

4.1.1 Hydrophone Receiving Response

Figure 4 shows the receiving response as a function of frequency for sensor #2 (CF lengthways). Two orientations were measured. Firstly with the acoustic pressure applied perpendicular to the face of the film in the 3 direction (Red) and secondly with the pressure applied along the width of the film parallel to the 2 direction (Black). Since the polyurethane is cylindrical, any effects on the acoustic propagation inside the sensor will be the same in all lateral directions. The two solid lines for each orientation show the response of opposite sides of the sensor. Ideally these should be the same but as can be seen there is a noticeable difference over all frequencies in both the 3 and 2 directions. For the 3 direction this difference is approximately 3 μV Pa^{-1} at 30 kHz and gradually decreases to 1 μVPa^{-1} at 100 kHz. In the 2 direction there is a constant difference of approximately 0.5 μVPa^{-1} over most of the frequencies with a crossover at around 40 kHz. The origin of these differences is unclear but could be due to variability in the resin/fibre ratio at various parts of the sensor that may have been introduce during the fabrication process. As mentioned earlier, there is also a slight offset of the sensor from the central plane but this is too small to account for the differences observed and would also not explain any variability in the 2 direction.

The red and black circles show the average of the two sides for both orientations. The triangles show the sensitivities for sensor #1 the plain SDT1 with no backing. It should be noted that this data was taken every 10 kHz compared to a 2 kHz spacing for sensor #2. As can be seen for frequencies less than 80 kHz the response of both samples have similar levels. At higher frequencies the plain film (Sensor #1) has approximately 3 μV Pa^{-1} higher response than Sensor #2.

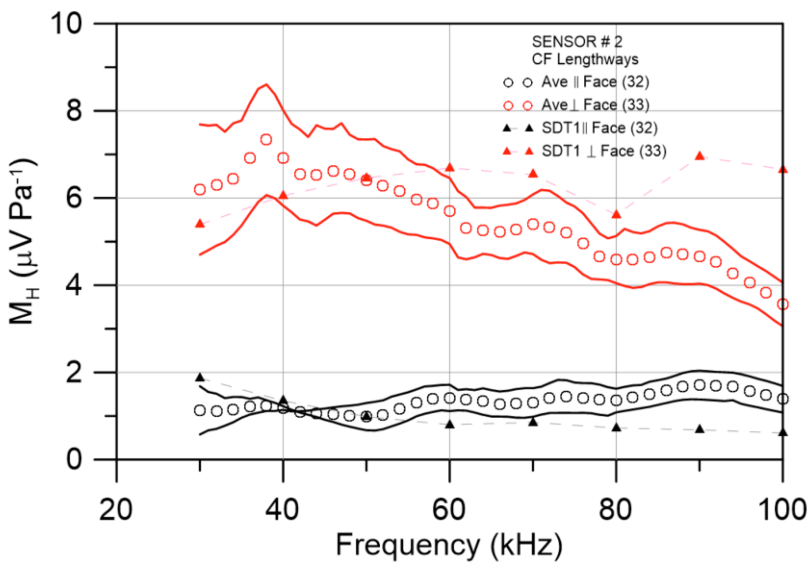

Figure 4. Sensitivity of Sensor#2 (CF lengthways) as a function of frequency for the 3 direction (red) and the 2 direction (black). Circles show the average of both sides. Solid lines show the response of both sides. Triangles show results for sensor #1 the plain SDT1 film with no backing material.

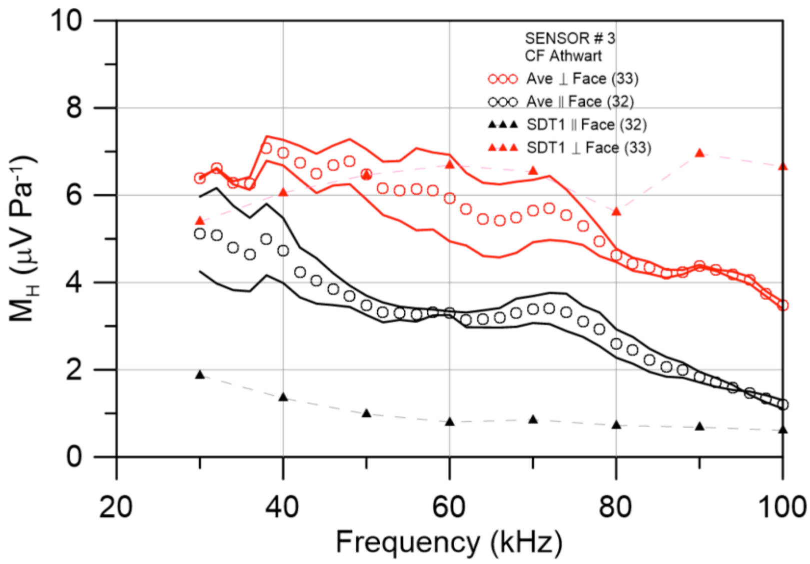

Figure 5. Sensitivity of Sensor#3 (CF athwart) as a function of frequency for the 3 direction (red) and the 2 direction (black). Circles show the average of both sides. Solid lines show the response of both sides. Triangles show results for sample#1 the plain SDT1 film with no backing material.

Figure 5 shows the receiving response as a function of frequency for sensor #3 (CF athwart). For this sample a clear increase in the sensitivity in the 2 direction is observed compared to sensor #2. The response of sensor #1 is shown as triangles. For the frequency range 30 kHz < f < 70 kHz the sensitivity in the 2 direction has been increased by a factor of approximately 2.5. Even for frequencies greater than 70 kHz the increase is significant. As was seen previously both sides of the film have different sensitivities but these differences are not the same as those measured in sensor #2. It should be noticed however that for frequencies above 80 kHz and below 40 kHz the sensor response is the same for both sides.

Figure 6a shows the ratio of the V_{33}:V_{32} responses of sensor #3 to #2. Sensor #2 with the carbon fibre running lengthways has a much higher 33 response than the 32 (approximately six times that of the 32 output up to 75 kHz). For sensor #3 however this ratio is significantly smaller with a ratio of just under 2 up to 90 kHz. Figure 6b shows the ratio of the 33 response (red) and the ratio of the 32 response (black) for sensor #2 and #3.

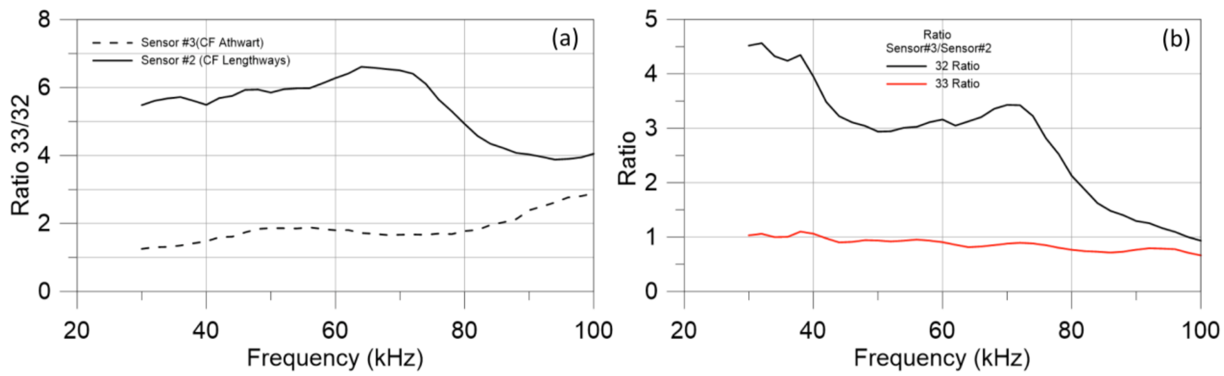

Figure 6. Sensitivity comparison of Sensors #2 and Sensor #3

The increase in response of sensor #3 in the 32 direction is very clear. In the 33 direction however the orientation of the CF has little effect. This difference could be attributed to the orientation of the carbon fibre that introduces an anisotropic Young's modulus in the substrate as discussed above in equation (2). As can be seen from equation (1) this will result an anisotropic voltage response.

4.1.2 Hydrophone Directivity

Figure 7 shows the directivity plots for sensors 1,2,3 and 4 for frequencies from 30 kHz to 100 kHz. The sensitivities at the centre and outer radius of the circle is -270 and -220 dB re 1V μPa^{-1} respectively. Sensor #4 is the biaxial +/- 45^o where the glass fibres are running +/- 45^o to the length of the film. For all sensors the flat face of the film (3 direction) is facing the sound source at 90^o and 270^o. Figure 7a shows the beam pattern for sensor #1 the plain SDT1 film with no backing. The directionality is very clear even down to 30 kHz. As mentioned above it was not possible to model the frequency dependence of this beam pattern using a conventional rigid baffle model (Matthews et al., 2013)

Figure 7c show the beam pattern for sensor #3 where the carbon fibres are parallel to the width of the film. As can be seen this sensor is omni-directional for all frequencies less than 50 kHz and is still reasonable up to 100 kHz. The side lobes observed for the plain film sensor #1 have been totally removed resulting in a beam pattern more indicative of a cylindrical hydrophone rather than a flat film. Figure 7b shows the beam pattern for sensor #2 (CF running parallel to the length). While the effects of the side lobes have been reduced they are still visible at all frequencies compared to sensor #3. Figure 7d shows the directionality of sensor #4 the bi-axial +/- 45^o sensor. The beam pattern for this sensor is similar to sensor #3 but not as omni-directional at higher frequencies.

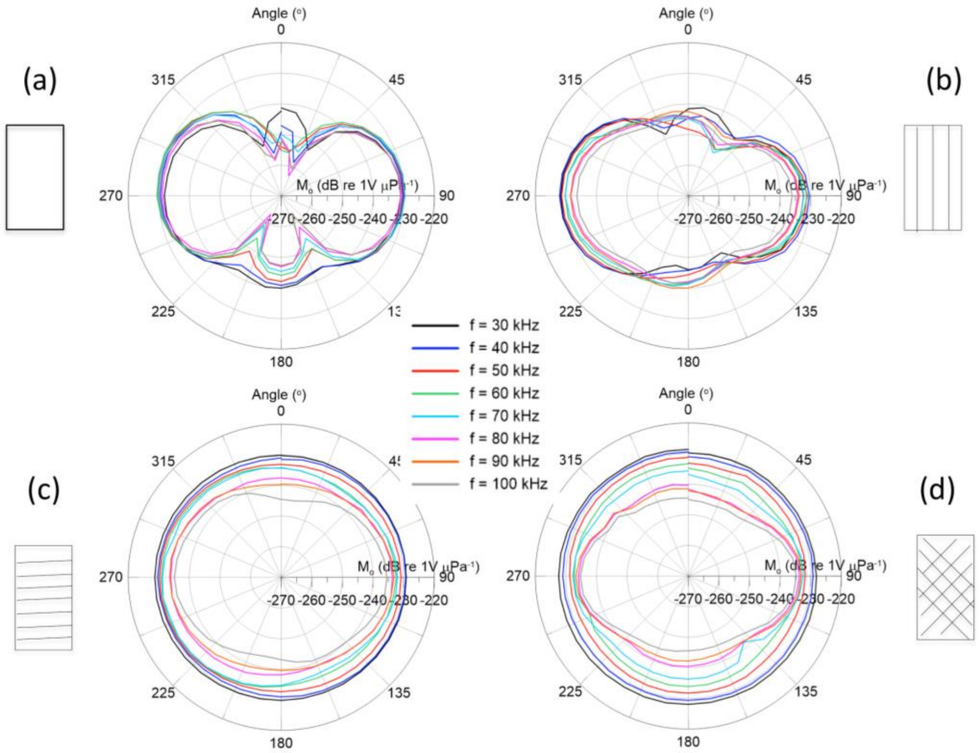

Figure 7. Directivity of sensors #1 (a), #2 (b), #3(c) and #4 (d) in dB re 1v/μPa. The flat face of the film (3 direction) is facing the sound source at 90° and 270°.

5. CONCLUSION

It has been shown that it is possible to control the directivity of a thick film PVDF hydrophone to produce an omnidirectional sensor up to 50 kHz. This was achieved by attaching the PVDF film to a thin substrate of carbon fibre with the fibres running parallel to the 2 direction (along the width) of the film. In doing so it was possible to increase the overall receiving response of the film in this direction. It is hypothesised that this is due to the suppression of the voltage contribution from V_{32} due to the influence of the high Young's modulus in the underlying substrate. This in turn reduces the stress coupling into the PVDF film in this direction. Since V_{33} is negative and V_{31} and V_{32} are positive a reduction in V_{32} results in an increase of the overall sensitivity of the sensor. Similar results were observed using glass fibre substrates but to a lesser extent.

By making the sensors cylindrical any angular refractive effects of the polyurethane remained constant for all angles (θ). As a result it was possible to make a direct comparison of the effect of various substrates on the sensor performance. Future work will focus on numerically modeling the sensors to get a better understanding of the anisotropic substrates and polyurethane.

ACKNOWLEDGEMENTS

The authors would like to acknowledge Ben Travaglione for his assistance and useful discussion.

REFERENCES

Bhat, J.J., Pillai, P.S. and Sridhar, C.S., 1995. Design and development of refined (3, 1) drive low-frequency piezofilm hydrophones. *The Journal of the Acoustical Society of America*, *97*(2), pp.1019-1022.

Holden, A.J., Parsons, A.D. and Wilson, A.E.J., 1983. Flexural disk hydrophones using polyvinylidene fluoride (PVDF) piezoelectric film: Desensitization with increasing hydrostatic pressure. *The Journal of the Acoustical Society of America*, *73*(5), pp.1858-1862.

Kawai, H., 1969. The piezoelectricity of poly (vinylidene fluoride). *Japanese Journal of Applied Physics*, *8*(7), p.975.

Kotian, K., Headings, L.M. and Dapino, M.J., 2013. Stress Averaging in PVDF Sensors for in-Plane Sinusoidal and Impact-Induced Stresses. *IEEE Sensors Journal*, *13*(11), pp.4444-4451.

Kharat, D.K., Mitra, S., Akhtar, S. and Kumar, V., 2007. Polymeric piezoelectric transducers for hydrophone applications. *Defence Science Journal*, *57*(1), p.7.

Matthews, D., Munyard, A. and Killeen, D., 2013. The effect of polyurethane encapsulant on the response of PVDF hydrophones in the frequency range from 30 kHz to 100 kHz. In *Proceedings of Acoustics*.

Moffett, M.B., Powers, J.M. and McGrath, J.C., 1986. A ρc hydrophone. *The Journal of the Acoustical Society of America*, *80*(2), pp.375-381.

Munyard, A., Matthews, D.N. and Killeen, D., 2012. The effect of backing material on the sensitivity of PVDF hydrophones at high frequencies. In *Proceedings of Acoustics*.

Ricketts, D., 1980. Electroacoustic sensitivity of composite piezoelectric polymer cylinders. *The Journal of the Acoustical Society of America*, *68*(4), pp.1025-1029.

Wang, H.W., Zhou, H.W., Gui, L.L., Ji, H.W. and Zhang, X.C., 2014. Analysis of effect of fiber orientation on Young's modulus for unidirectional fiber reinforced composites. *Composites Part B: Engineering*, *56*, pp.733-739.

Woodward, B. and Chandra, R.C., 1978. Underwater acoustic measurements on polyvinylidene fluoride transducers. *Active and Passive Electronic Components*, *5*(3), pp.149-157.